Direct observation of the particle exchange phase of photons

Konrad Tschernig
Max-Born-Institut
Chris Müller
Department of Physics and IRIS Adlershof, Humboldt-Universität zu Berlin, 12489 Berlin, Germany
Malte Smoor
Humboldt University of Berlin
Tim Kroh
Humboldt-Universität zu Berlin
Janik Wolters
Technical University of Berlin
Oliver Benson
Humboldt Universität zu Berlin Newtonstraße 15
Kurt Busch
Humboldt University of Berlin
Armando Perez-Leija (✉ Armando.Perez@mbi-berlin.de)
Max-Born-Institut

Research Article

Keywords: particle exchange, photons, bosonic

Posted Date: December 15th, 2020

DOI: https://doi.org/10.21203/rs.3.rs-124075/v1

Version of Record: A version of this preprint was published at Nature Photonics on June 3rd, 2021. See the published version at https://doi.org/10.1038/s41566-021-00818-7.

Direct observation of the particle exchange phase of photons

Konrad Tschernig[1,2*], Chris Müller[2,3*], Malte Smoor[3], Tim Kroh[2,3], Janik Wolters[4,5], Oliver Benson[2,3], Kurt Busch[1,2], Armando Pérez-Leija[1,2]

[1]Max-Born-Institut für Nichtlineare Optik und Kurzzeitspektroskopie
Max-Born-Straße 2A, 12489 Berlin, Germany
[2]Institut für Physik, Humboldt-Universität zu Berlin
Newtonstraße 15, 12489 Berlin, Germany
[3]IRIS Adlershof, Humboldt-Universität zu Berlin
Zum Großen Windkanal 6, 12489 Berlin, Germany
[4]Deutsches Zentrum für Luft- und Raumfahrt e.V. (DLR), Institute of Optical Sensor Systems
Rutherfordstraße 2, 12489 Berlin, Germany
[5]Technische Universität Berlin, 12489 Berlin, Institut für Optik und Atomare Physik,
Straße des 17. Juni 135, 10623 Berlin, Germany

Quantum theory stipulates that if two particles are identical in all physical aspects, the allowed states of the system are either symmetric or antisymmetric with respect to permutations of the particle labels. Experimentally, the symmetry of the states can be inferred indirectly from the fact that neglecting the correct exchange symmetry in the theoretical analysis leads to dramatic discrepancies with the observations. The only way to directly unveil the symmetry of the states for, say, two identical particles is through the interference of the two-particle state and the physically permuted one, and measuring the phase associated with the permutation process, the so-called particle exchange phase. Following this idea, we have measured the exchange phase of indistinguishable

photons, providing direct evidence of the bosonic character of photons.

In three spatial dimensions, quantum physics distinguishes between two fundamental types of particles, bosons and fermions (*1*). As a result, indistinguishable bosons satisfy the Bose-Einstein statistics and indistinguishable fermions obey the Fermi-Dirac statistics. Simply put, this means that fermions cannot occupy the same quantum state, as dictated by the Pauli exclusion principle (*2*), while bosons are allowed to 'condensate' into the same state (*3*). Quite remarkably, these distinctive characteristics are key ingredients that give form to all the existing elements and fields as we know them in the universe.

From a theoretical perspective, it has been postulated that the correct statistics for bosons and fermions can only be observed provided the associated states are symmetric and anti-symmetric, respectively (*4*). This means that, under permutations of the labels of any pair of particles, the allowed states of a system of N identical bosons must remain unchanged, $\hat{P}_{i,j}\,|N \text{ bosons}\rangle = |N \text{ bosons}\rangle$, while the states of a system of N identical fermions must undergo a sign change, $\hat{P}_{i,j}\,|N \text{ fermions}\rangle = -\,|N \text{ fermions}\rangle$ (*5*). Here, $\hat{P}_{i,j}$ represents the permutation operator that interchanges the labels of the i'th and j'th particle, where i and j are arbitrary.

Certainly, the (anti-)symmetric nature of identical particle states has very profound implications for quantum science and technology (*6*). In this respect, perhaps the most prominent example is the so-called Hong-Ou-Mandel effect (*7*), which gives rise to maximally mode-entangled two-photon states by interfering two indistinguishable photons (*7*). Importantly, the observation of mode-entanglement only depends on the symmetry of the two-photon wave function (*6*).

Quite recently, it has been realized that (anti-)symmetric multi-particle states belong to a very special set of quantum states referred to as decoherence-free subspaces (*8*), that is, quantum states that are immune to the impact of environmental noise. Even more importantly, it has been shown that quantum superpositions of indistinguishable states provide a natural control for the generation of noise-free entanglement (*9*), and they represent a source of quantum co-

herence, even when the associated particles are prepared independently (*10*). It is worth to remark that, contrary to what was thought in the past, the entanglement of identical particles is truly physical (*11*) and it is known to provide the metrological advantages for estimating phase shifts in systems of identical bosons (*12*).

Beyond explorations of the advantages offered by quantum indistinguishable particles, many authors have investigated the validity of the symmetrization postulate in a variety of experiments ranging from spectroscopy (*13, 14, 15*), via quantum chemistry (*16*) to ultracold atoms (*17*). Yet, in all those experiments the postulate has been demonstrated indirectly, e.g. by examining the absence of particular states which are forbidden by the postulate (*18, 19, 14, 20*). In physical terms, the (anti-)symmetrization of the states implies the existence of a definite relative phase between the constituent states (*21*). This concept is more intuitively illustrated for the particular case of two indistinguishable particles occupying two different spatial modes x and y with equal probability amplitude $1/\sqrt{2}$. Thus, the only possibility that satisfies the symmetrization postulate is

$$|\Psi\rangle = \frac{1}{\sqrt{2}} \left(|x\rangle\,|y\rangle + e^{i\phi_x}\,|y\rangle\,|x\rangle \right), \tag{1}$$

with $\phi_x = 0$ for bosons and $\phi_x = \pi$ for fermions. The argument ϕ_x is termed the *particle exchange phase* (EP) and, in principle, it is amenable to direct measurement (*22*). Clearly, such a measurement of the EP would reflect directly the fundamental physical symmetry of the associated states (*21*).

Experimentally, the only way to measure phase differences is via interferometry. That is, to observe the EP we have to superpose a reference state $|x\rangle\,|y\rangle$, with its physically permuted version $e^{i\varphi}\,|y\rangle\,|x\rangle$. However, care has to be exercised: Exchanging the position, or other physical properties, of two identical particles yields a final state exhibiting a phase factor φ composed not only of the EP but it also contains an extra phase shift ϕ_g whose origin is purely geomet-

ric (*23*). Essentially, the geometric phase is an observable phase accumulation that is acquired by the states of physical systems whose dynamic is cyclic, i.e., when the states return to their initial configuration (*24, 25*). In other words, when considering the actual experimental implementation of exchanging the states of two identical particles one cannot ignore the geometric phase associated with this exchange.

In this work, we report on the observation of the particle exchange phase for indistinguishable photons. For our experiments, we have implemented an interferometer that superposes a reference state of two indistinguishable photons occupying two spatial modes with its physically permuted version (*26*). Our direct measurements yield $\phi_x = (-0.04 \pm 0.07)$ rad, which imposes less stringent bounds on a possibly anomalous photon exchange phase than previous indirect measurements as reported in (*15, 27*). Concurrently, our observations reveal a geometric phase $\phi_g = \pi$, which is expected from a swap operation on identical particles (*28*).

Our experimental setup is based on the state-dependent-transport protocol as laid out in (*26*). It consists of two coupled Mach-Zehnder interferometers sharing the input ports and coupled to each other by a swap beam splitter (swap-BS), which is realized using a polarization beamsplitter (PBS), Fig. (1-a). Here, we use the convention that the PBS's reflect (transmit) vertically-polarized (horizontally-polarized) light. As input we launch two collinear orthogonally-polarized photons into port 1, which are routed to paths 1 and 2 using a PBS, yielding the state $|\leftrightarrow_1, \updownarrow_2\rangle$. Using a half-wave plate (HWP), we transform this latter state into $|\nearrow_1, \nwarrow_2\rangle$, which is a diagonally-anti-diagonally polarized two photon state on paths 1 and 2, respectively. Crucially, impinging the state $|\nearrow_1, \nwarrow_2\rangle$ onto the swap-BS generates the reference state $|\leftrightarrow_1, \updownarrow_4\rangle$ and a permuted version of it $|\updownarrow_3, \leftrightarrow_2\rangle$, Fig. (1-b). Notice we disregarded the contributions $|\leftrightarrow_1, \leftrightarrow_2\rangle$ and $|\updownarrow_3, \updownarrow_4\rangle$, where both photons are transmitted or reflected on the

swap-BS, in post-selection.

As required by the state-dependent-transport protocol, up to this point the two-particle states have not overlapped. Consequently, the total wave function lacks any meaningful symmetry property (*21*). We then use two 50-50 beamsplitters to overlap the reference and the permuted states. To obtain the relative phase we need a convenient observable for the interfered states such that its expectation value yields a cross-term whose argument is the total phase. This observable is found to be the combined photon coincidence rate between the four detectors at the outputs

$$\langle \hat{\Pi} \rangle \equiv \langle \hat{n}_1 \hat{n}_4 + \hat{n}_2 \hat{n}_3 - \hat{n}_1 \hat{n}_3 - \hat{n}_2 \hat{n}_4 \rangle = \frac{1}{2} \cos(\phi_1 + \phi_2 + \pi - \phi_x), \tag{2}$$

where ϕ_1 and ϕ_2 are two known reference phases, which are adjusted deterministically using the two mirrors in arms 1 and 2 attached to two piezo-elements. In Fig. (2) we present a detailed description of the complete interferometer implemented for our experiments, including the state preparation and the measurement stage.

The reference phases ϕ_1 and ϕ_2 are obtained by separately launching a diagonally-polarized, attenuated laser beam into the input-port 2 and taking the difference of the single-photon click-rates between the detectors $(\hat{n}_1, \hat{n}_2)$ and $(\hat{n}_3, \hat{n}_4)$ to give $\langle \hat{n}_2 - \hat{n}_1 \rangle = \frac{1}{2} \cos(\phi_1)$ and $\langle \hat{n}_3 - \hat{n}_4 \rangle = \frac{1}{2} \cos(\phi_2)$, see Fig. (3-a). Since the attenuated laser source has a small probability of emitting two photons (an unwanted contribution at this measurement stage) we discarded all detection events where two detectors clicked within a window of 400 ns.

In Eq. (2) we have included an additional phase π to account for the geometric phase contributed by the physical swap-operation on the two-photon states. Indeed, and as alluded to above, the relative phase between the states is not only determined by the particles' fundamental statistics ϕ_x, but also by the dynamic phase ϕ_d and the geometric phase ϕ_g, as defined by Aharonov and Anandan (*24*). In general, the physical swapping of the quantum states of two indistinguishable particles yields $\phi_g = \pi$, while the dynamic phase $\phi_d = 0$ vanishes (*29*).

To measure $\hat{\Pi}$ as a function of the total reference phase $(\phi_1 + \phi_2)$, we first send calibration photons to determine the actual phases ϕ_1 and ϕ_2. Next, we launch photon pairs (post-selected detection rate of ≈ 4200 pairs/min) and measure photon coincidences to obtain $\langle\hat{\Pi}\rangle$. By repeating this process and changing the voltages applied to the two piezo elements after each measurement, we collect the coincidences for several values of $(\phi_1 + \phi_2)$, as shown in Fig. (3-b). In order to exclude indeterministic thermal fluctuations of ϕ_1 and ϕ_2 we set the accumulation time for one measurement point to ≈ 1 seconds, which is much smaller than the time-scale (several hours to days) over which thermal phase drifts have been observed in our setup.

Notably, for the observable $\hat{\Pi}$ the losses, dark counts, and imperfect indistinguishability (86 $\pm$ 5 % in our case, where 100% corresponds to perfect indistinguishability) only contribute as a visibility reduction, and as an offset in the $\langle\hat{\Pi}\rangle$-signal, which is independent of ϕ_1 and ϕ_2. Since the particle exchange phase ϕ_x is given as a horizontal displacement of $\langle\hat{\Pi}\rangle$ along the $(\phi_1 + \phi_2)$-axis, our results are therefore robust against systematic errors due to experimental imperfections (*29*).

Fig. (3-c) depicts the measured coincidence rate, $\langle\hat{\Pi}\rangle$, for different values of $(\phi_1 + \phi_2)$ (blue dots). The data points are sorted into bins of width 0.1 radians, with respect to the sum $(\phi_1+\phi_2)$, and the mean value of the bins is calculated with the standard error as an uncertainty, Fig. (3-d). To model the measured data and to determine the phase experimentally we use a slight variation of Eq. (2), $\langle\hat{\Pi}\rangle = A\cos(\phi_1+\phi_2-\phi_x+\pi)+C$, where the amplitude A has to be positive and C describes a constant offset. Both constants characterize the combined effects of the brightness of the two-photon source, detection efficiencies, detector noise, distinguishability of the photon pairs and the integration times. As explained in (*29*) these effects do not contribute to a horizontal displacement of the signal (along the $(\phi_1 + \phi_2)$-axis) and, therefore, have no systematic impact on the obtained value for the EP ϕ_x. This feature makes the present interferometric

method robust against experimental imperfection. The fit (red solid line) in Fig. (3-d) reveals an exchange phase of $\phi_x = (-0.04 \pm 0.07)$ radians (95% confidence interval). This result includes an exchange phase of zero revealing the symmetric nature of the two-photon state and agrees with the expectation that photons are indeed bosons. Furthermore, this result demonstrates that it is crucial to consider the geometric phase of the swapping process, otherwise our measurements would lead to the erroneous conclusion that two-photon states are anti-symmetric.

It is interesting to note that many textbooks introduce the symmetrization postulate stating that quantum mechanical systems comprising N identical particles are either totally symmetric or anti-symmetric under the exchange of any pair of particles (*5, 30*). Such statement seems to imply that the physical situation must remain unaffected if the particles are physically exchanged. However, as demonstrated here, that is not the case, and our work will serve as reference to correctly address the symmetrization postulate. Furthermore, our results provide a first bound for a possibly non-vanishing exchange phase of photons, and is a starting point for precision measurements on tests of the symmetry of multi-particle wavefunctions.

We have developed an interferometric technique to directly measure the particle exchange phase of photons. To the best of our knowledge, this is the first direct interferometric measurement of the particle exchange phase. Within the margin of error our results confirm the symmetric nature of states that consist of two indistinguishable photons. Additionally, we demonstrated that it is crucial to consider the additional geometric and dynamic phase accumulated during the state-dependent transport protocol. Our implementation did not lead to the observation of any deviations from the expected exchange phase. Looking forward, our optical setup may be further improved and optimized towards enhanced accuracy. For example, a brighter and more stable photon pair source would allow for longer measurement times. Also the setup may be implemented using integrated and passively stable optical elements. In the next years a steady increase in accuracy and reduction of the bound for a non-vanishing exchange phase

can be achieved. Experimental tests of the exchange phase with other (Fermionic) particles would be highly attractive as well. Besides being, to the best of our knowledge, the first direct measurement of the exchange phase, our work puts forward an experimental technique to generate and certify spatially symmetrized two-photon states, which can find applications in transferring quantum information through random media (*8*), or to test entanglement of identical particles (*12*). Finally, our experiment is another example of how non-classical photon pair sources have now entered the field of precision measurements to investigate the validity of very fundamental laws of quantum mechanics (*31*).

References

1. J. M. Leinaas and J. Myrheim, "On the theory of identical particles," *Il Nuovo Cimento B (1971-1996)*, vol. 37, pp. 1–23, Jan 1977.

2. W. Pauli, "Über den Zusammenhang des Abschlusses der Elektronengruppen im Atom mit der Komplexstruktur der Spektren," *Zeitschrift fur Physik*, vol. 31, pp. 765–783, Feb. 1925.

3. K. B. Davis, M. O. Mewes, M. R. Andrews, N. J. van Druten, D. S. Durfee, D. M. Kurn, and W. Ketterle, "Bose-einstein condensation in a gas of sodium atoms," *Phys. Rev. Lett.*, vol. 75, pp. 3969–3973, Nov 1995.

4. A. M. L. Messiah and O. W. Greenberg, "Symmetrization postulate and its experimental foundation," *Phys. Rev.*, vol. 136, pp. B248–B267, Oct 1964.

5. J. J. Sakurai and J. Napolitano, *Modern Quantum Mechanics*. Cambridge University Press, 2 ed., 2017.

6. I. Walmsley, "Quantum interference beyond the fringe," *Science*, vol. 358, no. 6366, pp. 1001–1002, 2017.

7. C. K. Hong, Z. Y. Ou, and L. Mandel, "Measurement of subpicosecond time intervals between two photons by interference," *Phys. Rev. Lett.*, vol. 59, pp. 2044–2046, Nov 1987.

8. A. Perez-Leija, D. Guzmán-Silva, R. d. J. León-Montiel, M. Gräfe, M. Heinrich, H. Moya-Cessa, K. Busch, and A. Szameit, "Endurance of quantum coherence due to particle indistinguishability in noisy quantum networks," *npj Quantum Information*, vol. 4, no. 1, p. 45, 2018.

9. F. Nosrati, A. Castellini, G. Compagno, and R. Lo Franco, "Robust entanglement preparation against noise by controlling spatial indistinguishability," *npj Quantum Information*, vol. 6, no. 1, p. 39, 2020.

10. A. Castellini, R. Lo Franco, L. Lami, A. Winter, G. Adesso, and G. Compagno, "Indistinguishability-enabled coherence for quantum metrology," *Phys. Rev. A*, vol. 100, p. 012308, Jul 2019.

11. J. Sperling, A. Perez-Leija, K. Busch, and I. A. Walmsley, "Quantum coherences of indistinguishable particles," *Phys. Rev. A*, vol. 96, p. 032334, Sep 2017.

12. B. Morris, B. Yadin, M. Fadel, T. Zibold, P. Treutlein, and G. Adesso, "Entanglement between identical particles is a useful and consistent resource," *Phys. Rev. X*, vol. 10, p. 041012, Oct 2020.

13. R. C. Hilborn and C. L. Yuca, "Spectroscopic test of the symmetrization postulate for spin-0 nuclei," *Phys. Rev. Lett.*, vol. 76, pp. 2844–2847, Apr 1996.

14. G. Modugno, M. Inguscio, and G. M. Tino, "Search for small violations of the symmetrization postulate for spin-0 particles," *Phys. Rev. Lett.*, vol. 81, pp. 4790–4793, Nov 1998.

15. D. English, V. V. Yashchuk, and D. Budker, "Spectroscopic test of bose-einstein statistics for photons," *Phys. Rev. Lett.*, vol. 104, p. 253604, Jun 2010.

16. S. Ospelkaus, K.-K. Ni, D. Wang, M. H. G. de Miranda, B. Neyenhuis, G. Quéméner, P. S. Julienne, J. L. Bohn, D. S. Jin, and J. Ye, "Quantum-state controlled chemical reactions of ultracold potassium-rubidium molecules," *Science*, vol. 327, no. 5967, pp. 853–857, 2010.

17. K. Levin, A. L. Fetter, and D. M. Stamper-Kurn, *Ultracold Bosonic and Fermionic Gases*. Cambridge University Press, 1 ed., 2012.

18. E. Ramberg and G. A. Snow, "Experimental limit on a small violation of the pauli principle," *Phys. Lett. B*, vol. 238, p. 438, Nov. 1990.

19. M. de Angelis, G. Gagliardi, L. Gianfrani, and G. M. Tino, "Test of the symmetrization postulate for spin-0 particles," *Phys. Rev. Lett.*, vol. 76, pp. 2840–2843, Apr 1996.

20. D. DeMille, D. Budker, N. Derr, and E. Deveney, "Search for exchange-antisymmetric two-photon states," *Phys. Rev. Lett.*, vol. 83, pp. 3978–3981, Nov 1999.

21. R. Mirman, "Experimental meaning of the concept of identical particles," *Il Nuovo Cimento B (1971-1996)*, vol. 18, no. 1, pp. 110–122, 1973.

22. P. Landshoff and H. P. Stapp, "Parastatistics and a unified theory of identical particles," *Ann. of Phys.*, vol. 45, p. 72, Jan 1967.

23. A. Peres, *Quantum Theory: Concepts and Methods*. Springer, Dordrecht, 1 ed., 2002.

24. Y. Aharonov and J. Anandan, "Phase change during a cyclic quantum evolution," *Phys. Rev. Lett.*, vol. 58, pp. 1593–1596, Apr 1987.

25. K. Wang, S. Weimann, S. Nolte, A. Perez-Leija, and A. Szameit, "Measuring the aharonov–anandan phase in multiport photonic systems," *Opt. Lett.*, vol. 41, pp. 1889–1892, Apr 2016.

26. C. F. Roos, A. Alberti, D. Meschede, P. Hauke, and H. Häffner, "Revealing quantum statistics with a pair of distant atoms," *Phys. Rev. Lett.*, vol. 119, p. 160401, Oct 2017.

27. B. Altschul, "Testing photons' bose-einstein statistics with compton scattering," *Phys. Rev. D*, vol. 82, p. 101703, Nov 2010.

28. S. J. van Enk, "Exchanging identical particles and topological quantum computing," 2018.

29. "See supporting material,"

30. A. Messiah, *Quantum Mechanics*. Dover, 1 ed., 1999.

31. U. Sinha, C. Couteau, T. Jennewein, R. Laflamme, and G. Weihs, "Ruling out multi-order interference in quantum mechanics," *Science*, vol. 329, no. 5990, pp. 418–421, 2010.

Acknowledgments

The images of the experimental setup were created with the 3DOptix optical design tool. We thank the 3DOptix-Team, who kindly allowed the use of these images in this article. The authors thank PicoQuant GmbH for providing the MultiHarp 150. **Funding** C.M. T.K. and O.B. acknowledge support by the German Research Foundation (DFG) Collaborative Research Center (CRC) SFB 787 project C2 and the German Federal Ministry of Education and Research (BMBF) with the project Q.Link.X. **Author contributions:** A.P.L., K.T., O.B. and K.B. initiated the study and guided the work. K.T., C.M., T.K., M.S. and J.W. designed the interferometer. M.S., C.M. and T.K. set up the interferometer, C.M. and M.S. performed the optical measure-

ments. C.M. and K.T. analyzed and interpreted the experimental data. K.T. and A.P.L. developed the theory. K.T., C.M. and A.P.L. wrote the manuscript with input from all coauthors. **Competing interests:** None declared. **Data and materials availability:** All data needed to evaluate the conclusions in this paper are available in the manuscript and in the supplementary materials.

Supplementary Material

Supplementary Text

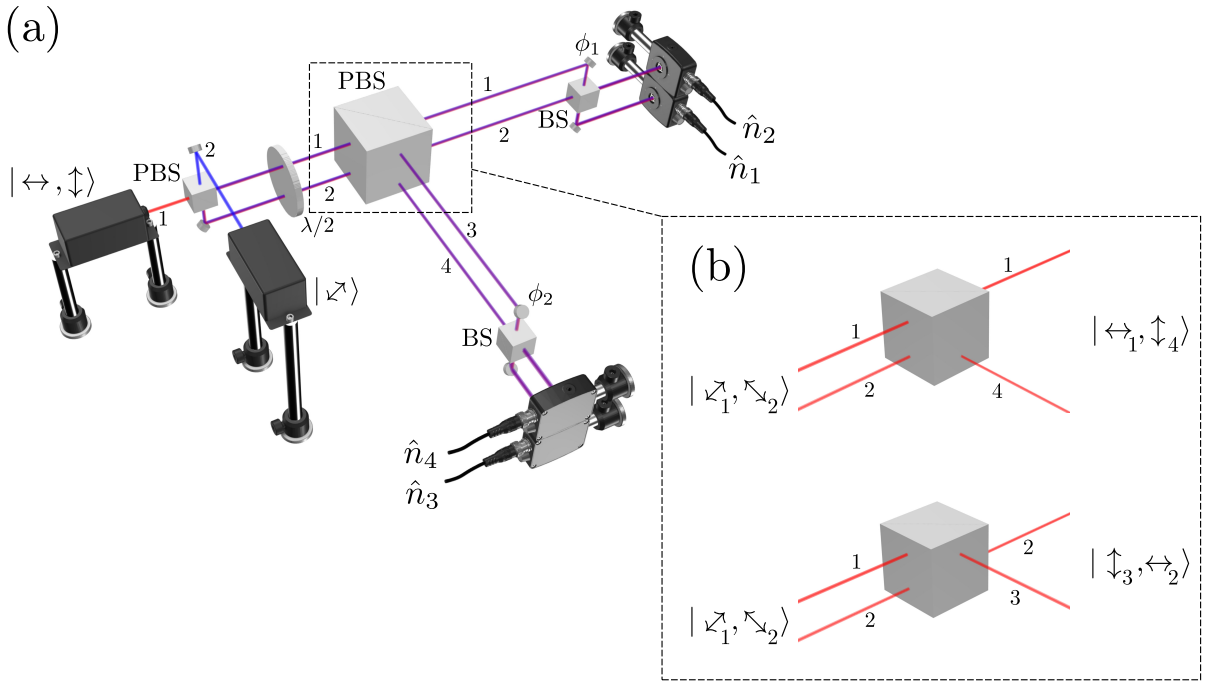

Figure 1: **(a)** Conceptual sketch of the interferometric setup. In the first measurement step, a diagonally-polarized attenuated laser beam is incident on input-port 2 (blue beam) and split 50:50 on the first PBS. The $\lambda/2$-waveplate brings the separate beams 1 and 2 back into diagonal polarization and they are again split with a 50:50 ratio on the second PBS. The beams acquire a phase-difference ϕ_1 (ϕ_2) between the paths 1 and 2 (3 and 4) and after recombination on the non-polarizing beam splitters we observe typical Mach-Zehnder interference fringes in the differences of the single-photon counts. In the second stage, two indistinguishable photons in orthogonal polarization are injected simultaneously into input-port 1 (red beam). Accordingly, they are separated at the first PBS and rotated to (anti-)diagonal polarization at the $\lambda/2$-waveplate. At the second PBS we consider two possible paths of the two-photon state. **(b)** One path where the photon in beam 1 is transmitted and the photon in beam 2 is reflected and the other path, where the photon in beam 1 is reflected and the photon in beam 2 is transmitted. Both possible paths contribute to the coincidence rates between detectors in the (1,2)-arm and the (3,4)-arm. The interferometric superposition of these two paths, ultimately reveals the exchange phase of photons.

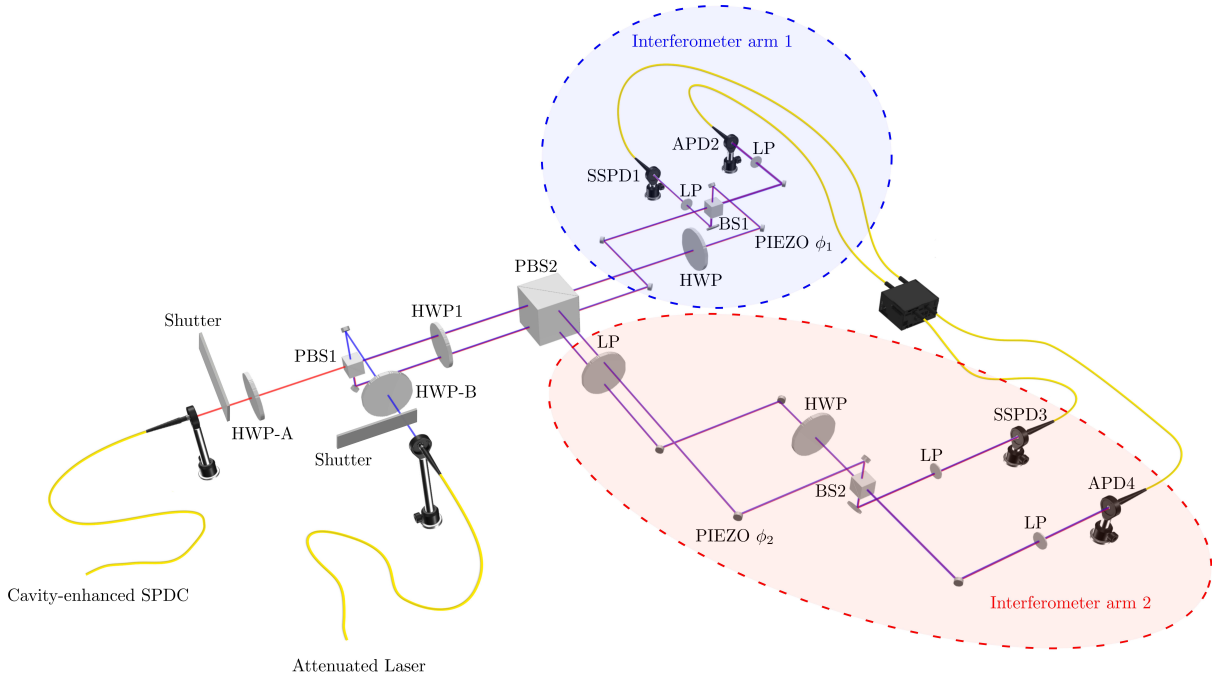

Figure 2: Complete interferometer setup. Indistinguishable photon pairs (red line) are launched into the interferometer (post-selected pair detection rate of ≈ 4200 pairs/min) using a polarization maintaining single mode fiber. The half-wave-plate-A (HWP-A) rotates the polarization of the photons to horizontal/vertical so that PBS1 splits them deterministically into two paths, as required by state-dependent transport protocol. A linear polarizer in the interferometer arm 2 is used to suppress the photons reflected at PBS2 with the undesired polarization. Both interferometer arms contain a mirror attached to a piezo-element to enable the deterministic control of the reference phases ϕ_1 and ϕ_2. A periscope in each arm combines the different heights. Due to the orientation of the mirrors in the periscopes, the polarization of photons in the upper path changes with respect to photons in the lower path. This is compensated by an additional HWP so that the two paths can interfere at the beam splitters BS1 and BS2. Linear polarizers (LP) after each output of BS1 and BS2 filter out photons with an undesired polarization. The photons are collected into single mode fibers – which also facilitates the optimal alignment of the optical paths – and guided to the individual detectors. Each arm is monitored by one avalanche photodiode (APD) and one superconducting single photon detector (SSPD), in order to maintain the symmetry between the interferometer arms. We correlate the detector signals with a time tagging module (PicoQuant MultiHarp 150). The second input port (blue line) of the interferometer connects the attenuated laser beam with the interferometer. HWP-B rotates the polarization of the beam to diagonal polarization, leading to an equal splitting ratio at PBS1. Finally, automated mechanical shutters at the input ports control whether the photon pairs or the attenuated laser are sent into the interferometer.

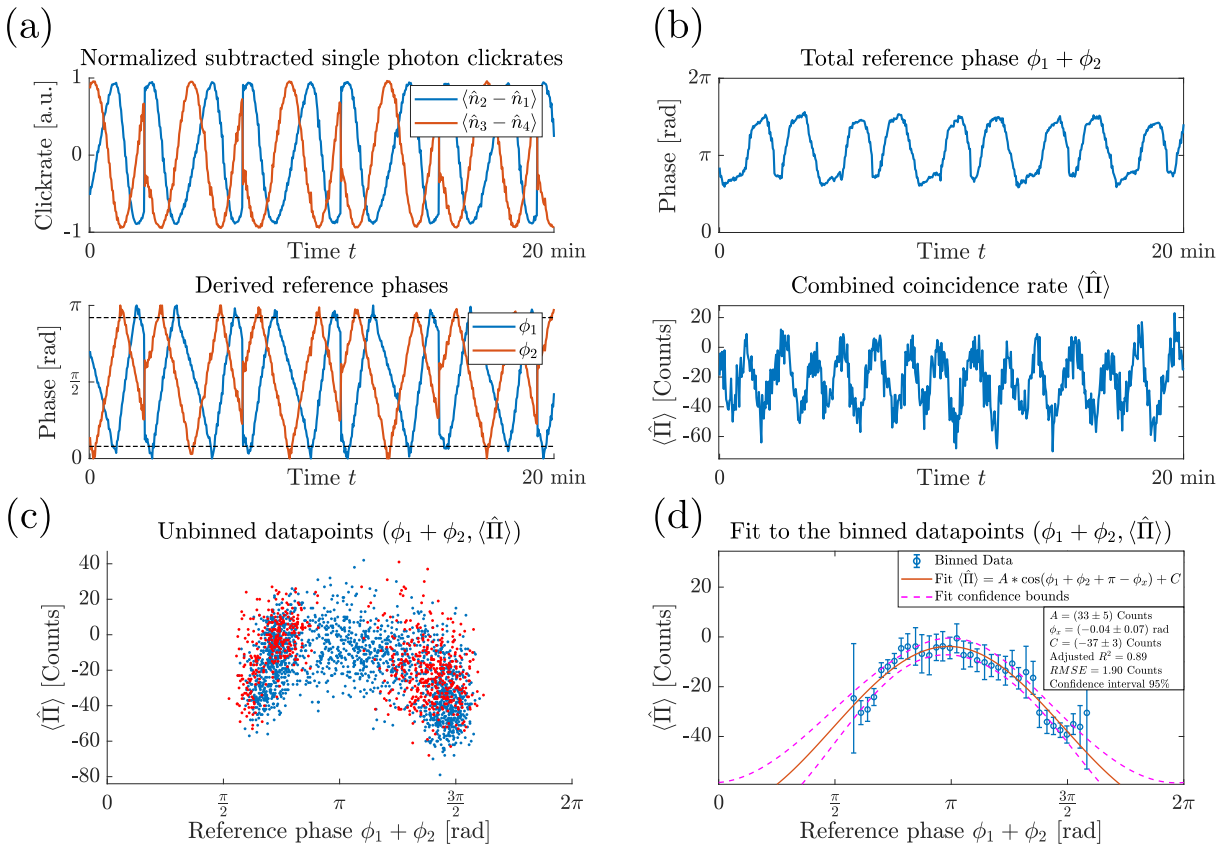

Figure 3: Measurement results. **(a)** Mach-Zehnder interference fringes observed over a time interval of 20 min, while the attenuated laser is fed into the setup. On the top we show the evolution of the differences of the normalized single-photon click-rates $\langle \hat{n}_2 - \hat{n}_1 \rangle$ (blue curve) and $\langle \hat{n}_3 - \hat{n}_4 \rangle$ (red curve) while changing the voltage applied to the piezo-elements. Note, that the discontinuous jumps correspond to the points where the applied saw-tooth voltage signal reverts to its minimum. From these measurements we obtain the corresponding reference phases ϕ_1 and ϕ_2 (bottom). **(b)** Total reference phase (top) and combined coincidence rate $\langle \hat{\Pi} \rangle$ (bottom) as they evolve in time. **(c)** Scatter-plot of all measured value pairs $(\phi_1 + \phi_2, \langle \hat{\Pi} \rangle)$ ($\approx$ 90 min measurement time in total). Since the slope of $\cos(\phi_{1(2)})$ vanishes at $\phi_{1(2)} = 0, \pi$, the associated uncertainty in the estimation of ϕ_1 and ϕ_2 diverges at these points. Therefore we consider only data points where ϕ_1 and ϕ_2 are within an interval of $[t, \pi - t]$ with $t = 0.25$ rad (blue points). This interval is also indicated by the dashed horizontal lines in (a). **(d)** We sort the data points into bins with respect to the total reference phase and perform a least-square error fit of $\langle \hat{\Pi} \rangle = A \cos(\phi_1 + \phi_2 + \pi - \phi_x) + C$, which yields $\phi_x = (-0.04 \pm 0.07)$ rad (95% confidence interval, adjusted $R^2 = 0.89$, $RMSE = 1.9$ Counts) and confirms the symmetry of the two-photon wavefunction.

Figures

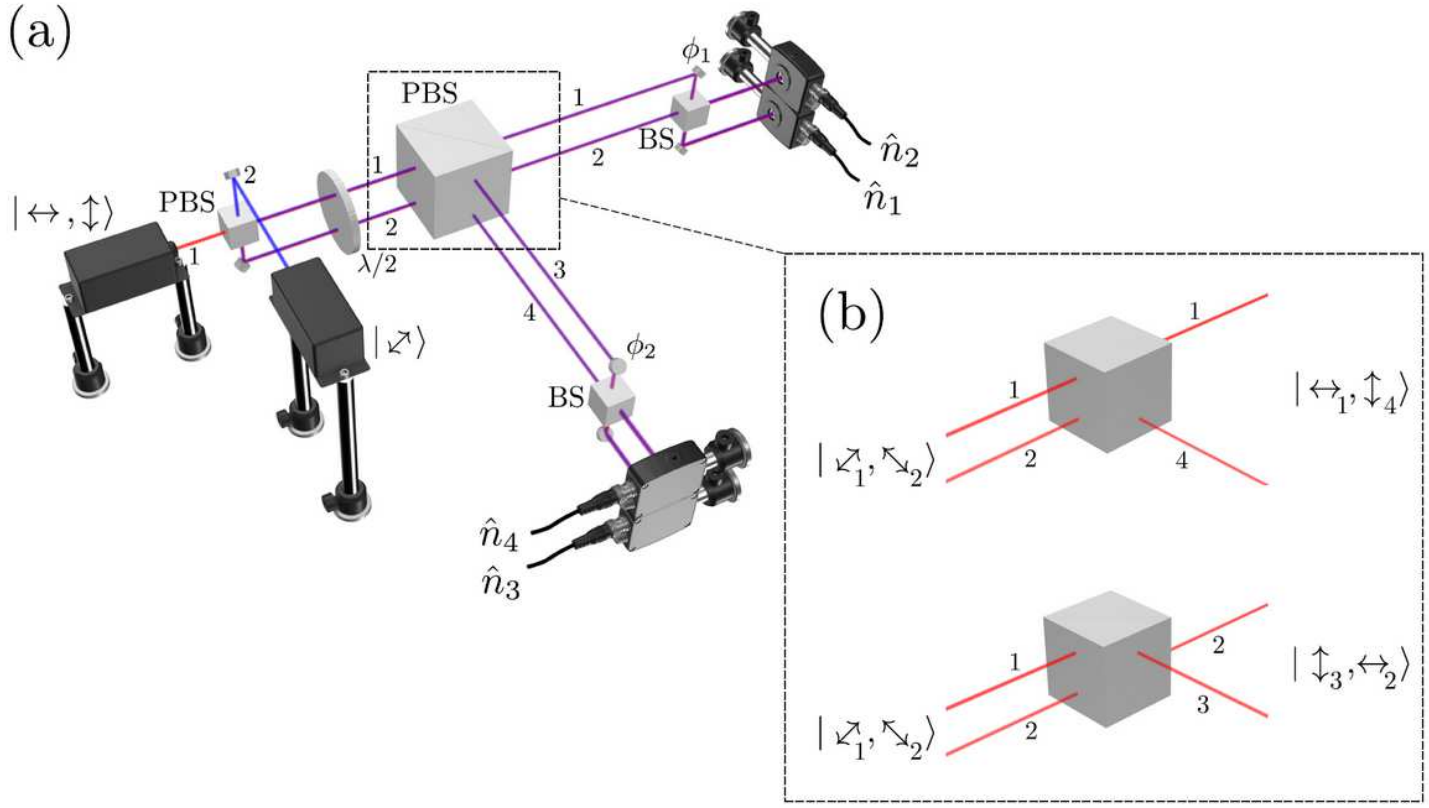

Figure 1

(a) Conceptual sketch of the interferometric setup. In the first measurement step, a diagonally-polarized attenuated laser beam is incident on input-port 2 (blue beam) and split 50:50 on the first PBS. The λ/2-waveplate brings the separate beams 1 and 2 back into diagonal polarization and they are again split with a 50:50 ratio on the second PBS. The beams acquire a phase-difference 1 (2) between the paths 1 and 2 (3 and 4) and after recombination on the non-polarizing beam splitters we observe typical Mach-Zehnder interference fringes in the differences of the single-photon counts. In the second stage, two indistinguishable pho tons in orthogonal polarization are injected simultaneously into input-port 1 (red beam). Accordingly, they are separated at the first PBS and rotated to (anti-)diagonal polarization at the λ/2-waveplate. At the second PBS we consider two possible paths of the two-photon state. (b) One path where the photon in beam 1 is transmitted and the photon in beam 2 is reflected and the other path, where the photon in beam 1 is reflected and the photon in beam 2 is transmit ted. Both possible paths contribute to the coincidence rates between detectors in the (1,2)-arm and the (3,4)-arm. The interferometric superposition of these two paths, ultimately reveals the exchange phase of photons.

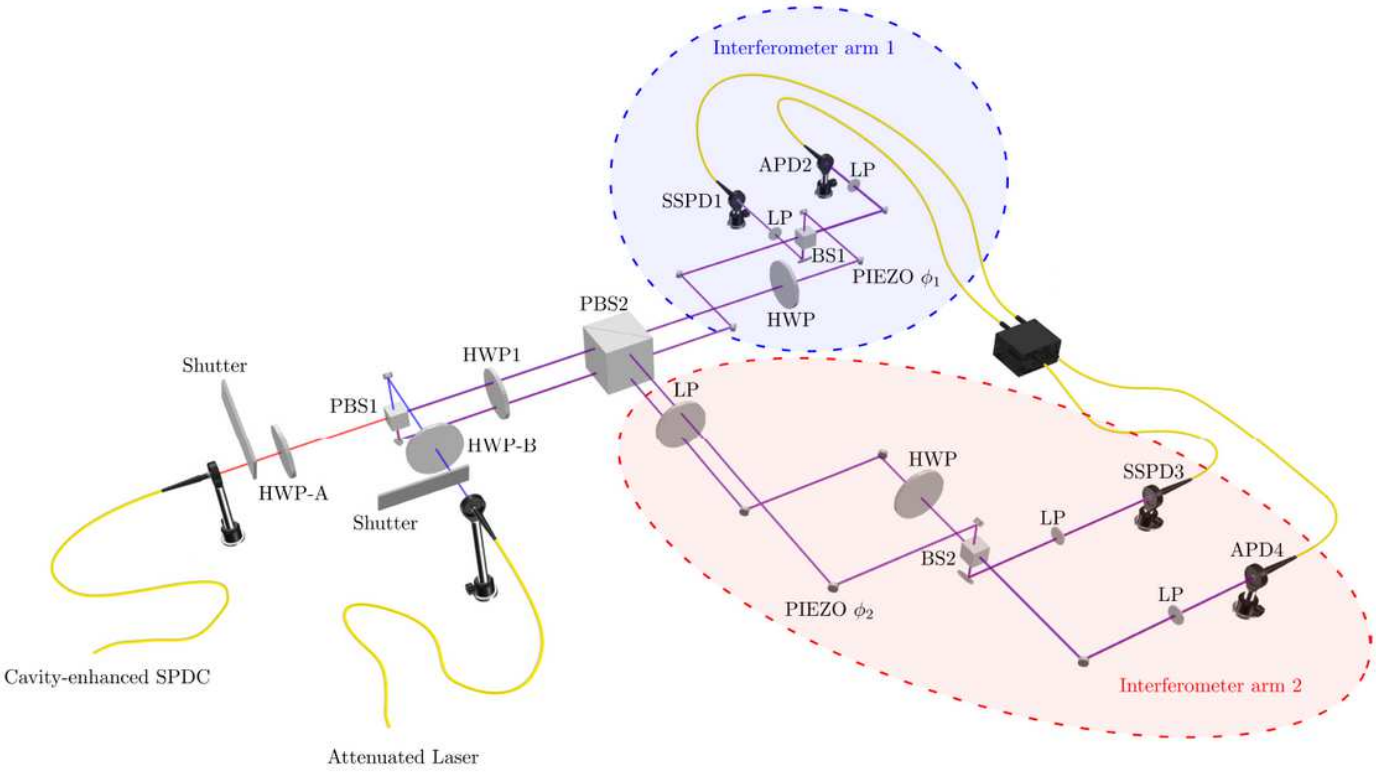

Figure 2

Complete interferometer setup. Indistinguishable photon pairs (red line) are launched into the interferometer (post-selected pair detection rate of ≈ 4200 pairs/min) using a polarization maintaining single mode fiber. The half-wave-plate-A (HWP-A) rotates the polarization of the photons to horizontal/vertical so that PBS1 splits them deterministically into two paths, as required by state-dependent transport protocol. A linear polarizer in the interferometer arm 2 is used to suppress the photons reflected at PBS2 with the undesired polarization. Both interferometer arms contain a mirror attached to a piezo-element to enable the deterministic control of the reference phases 1 and 2. A periscope in each arm combines the different heights. Due to the orientation of the mirrors in the periscopes, the polarization of photons in the upper path changes with respect to photons in the lower path. This is compensated by an additional HWP so that the two paths can interfere at the beam splitters BS1 and BS2. Linear polarizers (LP) after each output of BS1 and BS2 filter out photons with an undesired polarization. The photons are collected into single mode fibers – which also facilitates the optimal alignment of the optical paths – and guided to the individual detectors. Each arm is monitored by one avalanche photodiode (APD) and one superconducting single photon detector (SSPD), in order to maintain the symmetry between the interferometer arms. We correlate the detector signals with a time tagging module (PicoQuant MultiHarp 150). The second input port (blue line) of the interferometer connects the attenuated laser beam with the interferometer. HWP-B rotates the polarization of the beam to diagonal polarization, leading to an equal splitting ratio at PBS1. Finally, automated mechanical shutters at the input ports control whether the photon pairs or the attenuated laser are sent into the interferometer.

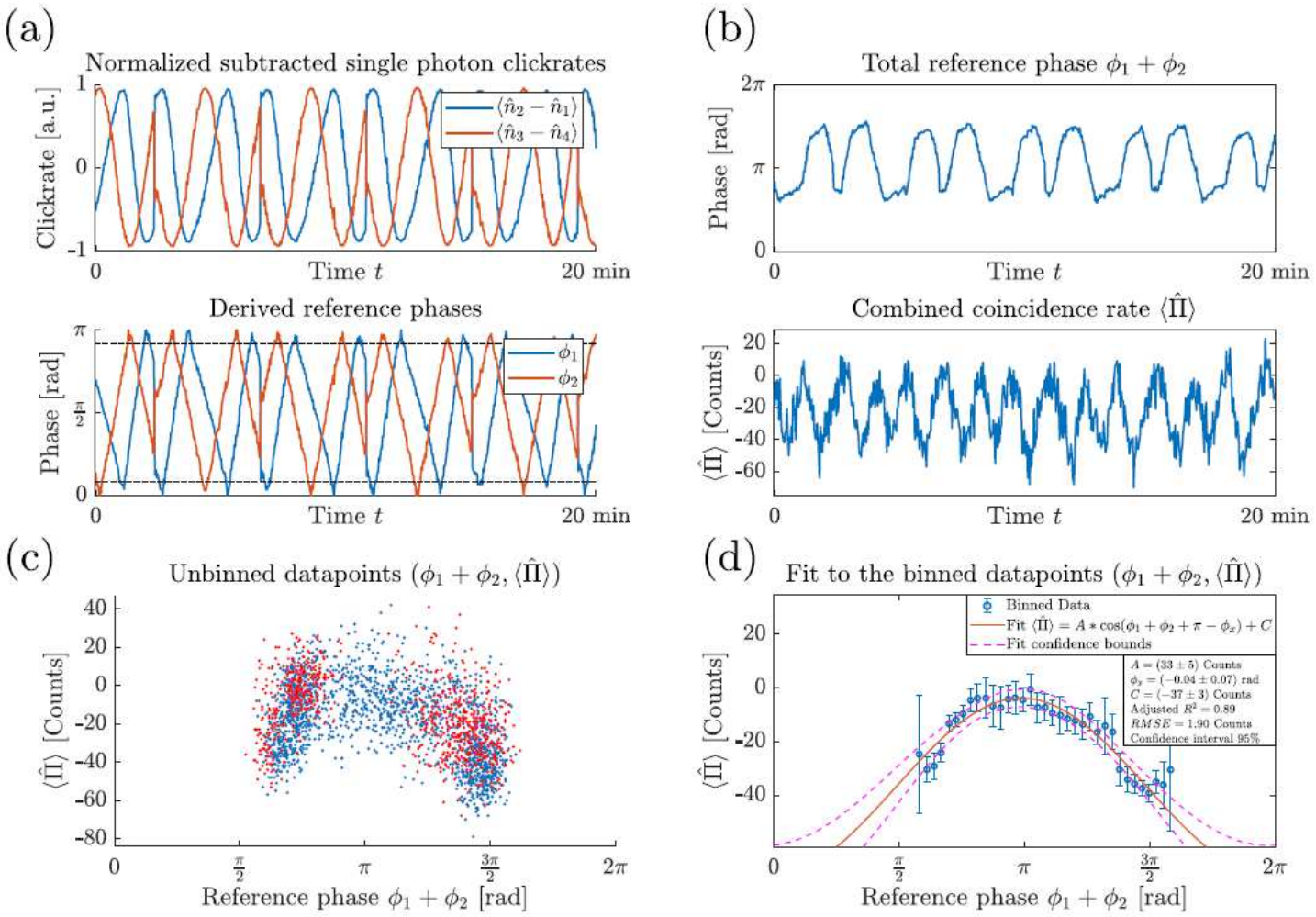

Figure 3

Measurement results. (a) Mach-Zehnder interference fringes observed over a time interval of 20 min, while the attenuated laser is fed into the setup. On the top we show the evolution of the differences of the normalized single-photon click-rates ⟨n̂2 − n̂1⟩ (blue curve) and ⟨n̂3 − n̂4⟩ (red curve) while changing the voltage applied to the piezo-elements. Note, that the discontinuous jumps correspond to the points where the applied saw-tooth voltage signal reverts to its minimum. From these measurements we obtain the corresponding reference phases ϕ1 and ϕ2 (bottom). (b) Total reference phase (top) and combined coincidence rate ⟨Π̂⟩ (bottom) as they evolve in time. (c) Scatter-plot of all measured value pairs (ϕ1 + ϕ2, ⟨Π̂⟩) (≈ 90 min measurement time in total). Since the slope of cos(ϕ1(2)) vanishes at ϕ1(2) = 0, π, the associated uncertainty in the estimation of ϕ1 and ϕ2 diverges at these points. Therefore we consider only data points where ϕ1 and ϕ2 are within an interval of [t, π − t] with t = 0.25 rad (blue points). This interval is also indicated by the dashed horizontal lines in (a). (d) We sort the data points into bins with respect to the total reference phase and perform a least-square error fit of ⟨Π̂⟩ = A cos(ϕ1 + ϕ2 + π − ϕx) + C, which yields ϕx = (−0.04 ± 0.07) rad (95% confidence interval, adjusted R2 = 0.89, RMSE = 1.9 Counts) and confirms the symmetry of the two-photon wavefunction.

Supplementary Files

This is a list of supplementary files associated with this preprint. Click to download.

- SI.pdf